Int. J. Heat Mass Transfer. Vol. 36, No. 6, pp. 1693–1700, 1993
Printed in Great Britain

0017-9310/93 \$6.00+0.00
Pergamon Press Ltd

Heat transfer and hydraulic drag in helical channels in gas flow

J. VILEMAS, P. POŠKAS, V. ŠIMONIS and V. ŠUKYS
Lithuanian Energy Institute, Kaunas, 3684, Lithuania

(*Received* 26 *November* 1991)

Abstract—Experimental results are given for heat transfer from convex and concave walls and for hydraulic drag in hydrodynamically and thermally stabilized air flow in rectangular helical channels over a wide range of operating conditions ($Re = 10^2$–2×10^5) and geometric parameters ($D/h = 5.5$–84.2, $b/h = 2.4$–18.5). It is established that, with an increase in the channel curvature, heat transfer from the concave wall is enhanced, whereas that from the convex wall is reduced, and a transition to turbulent flow on both walls occurs at different Reynolds numbers, which are larger than those in a straight channel, and has different lengths. Applying artificial roughness to the convex surface is shown to allow its heat transfer enhancement even to the level of heat transfer from the concave surface. Correlations are obtained for the critical Reynolds numbers at which the transition from laminar-vortex to turbulent flow occurs, for heat transfer from separate walls and for hydraulic drag in the helical channels.

1. INTRODUCTION

ONE PROMISING method of enhancing convective heat transfer is the action of mass centrifugal forces on flow of a heat transfer agent. This is realized in curvilinear (including helical) channels, frequently encountered in various heat exchangers, in cooling and heating systems, in nuclear reactors, in heat engines, etc. The complex character of flow and heat transfer in such channels with the interaction between the main axial motion and secondary flows, originating at certain operating conditions, mainly calls for an experimental method of study. Although a good deal of attention has been given to thermohydraulic investigations in curvilinear channels, the results obtained refer primarily to average characteristics, i.e. to the length- and perimeter-averaged heat transfer and hydraulic drag or only to length-averaged parameters [1, 2].

The local heat transfer over the channel length and perimeter has been studied to a much lesser extent. Data have been acquired mostly for very short curvilinear rectangular channels [3–6] and only refs. [2, 7–9] report results for longer curved (including helical [7–9]) channels. These studies demonstrate a considerable difference in heat transfer from the separate surfaces of the curvilinear channels; thus, ref. [2] established that heat transfer from a concave surface is twice as large as that from a convex surface, whereas heat transfer from an end surface is greater by 2.4 times. However, there are no correlations accounting for the effect of curvature and other geometric characteristics on the local heat transfer in curvilinear channels.

The present study presents experimental results for the local heat transfer from convex and concave surfaces and for the hydraulic drag of helical rectangular channels over a wide range of operating conditions ($Re = 10^2$–2×10^5) and geometric parameters ($D/h = 5.5$–84.2 and $b/h = 2.4$–18.5), as well as data for the heat transfer enhancement in a helical channel with a rough convex surface in hydrodynamically and thermally stabilized air flow.

2. INVESTIGATION TECHNIQUE

Investigations were performed on an open-type aerodynamic set-up. The test section represented a channel (Fig. 1(a)) formed by outer calorimetric stainless steel tube (1) with a 38.1 mm outer diameter, a 1.0 mm wall thickness, a 720 mm length and by replaceable textolite worm insertion (2), closely adjoining the outer tube, with stainless steel smooth or rough calorimetric 0.1-mm-thick foil (3) wound round the insertion groove. Thus, a helical rectangular channel with concave and convex heat transfer surfaces was produced. The use of the textolite worm with the foil allowed heat transfer to be determined only for the convex or concave main lateral surfaces of the channel (excluding the end surfaces).

The relative length of the helical channel constituted $l/d_e \gtrsim 80$ and the initial section of hydrodynamic stabilization of the length $x/d_e \gtrsim 20$ was straight annular. The calorimetric surfaces of the channel were heated by direct electric current. The channel wall temperature was measured with copper–constantan thermocouples (4) mounted lengthwise in 10 sections on the non-wetted sides of the calorimetric surfaces in the middle of the spacing between neighbouring fins. A detailed description of the test section is given in ref. [10].

To enhance heat transfer from the convex surface of the helical channel, use was made of the rough foil (Fig. 1(b)) with a three-dimensional artificial rough-

NOMENCLATURE

b	mean channel width
c_p	heat capacity
D	mean curvature diameter
d_1, d_2	diameters of wetted lateral surfaces of the channel and of the inner and outer tubes of the annulus, respectively
d_e	equivalent channel diameter
F	heat transfer surface
f	area of channel cross-section
h	channel height
k	roughness element height
l, x	length in the axial direction of channels
Nu	Nusselt number, $\alpha 2h/\lambda$
Pr	Prandtl number, $\mu c_p/\lambda$
q	heat flux density
Re	Reynolds number for analysing heat transfer, $u_f 2h/\nu$, and hydraulic drag, $u_f d_e/\nu$
$\overline{St}$	mean Stanton number, $(Nu_1 F_1 + Nu_2 F_2)/((F_1+F_2) Re\, Pr)$
s	channel swirling step
T	temperature
u	longitudinal velocity
u_*	dynamic velocity, $\sqrt{(\tau_w/\rho)}$
u^+	dimensionless velocity, u/u_*
y	distance from the wall
y^+	dimensionless distance, yu_*/ν.

Greek symbols

α	heat transfer coefficient
δ	fin thickness
λ	thermal conductivity
μ	dynamic viscosity
ν	kinematic viscosity
ξ	hydraulic drag
Π	channel perimeter
ρ	density
τ	shear stress
φ	mean angle of channel swirling.

Subscripts

0	straight channel
1	convex surface, inner tube of the annulus
2	concave surface, outer tube of the annulus
cr	critical value
f	in flow
L	laminar
T	turbulent
t	in the tube
w	at the wall.

ness in the form of tetrahedral pyramids. Such roughness is conservative to the direction of the heat transfer agent flow onto the roughness elements. The height of the roughness elements ($k = 0.2$ mm) was selected on the basis of the optimum conditions for the heat transfer enhancement in annuli [11].

Investigations were carried out in nine smooth and one rough (with a rough convex surface) helical channels with geometric characteristics presented in Table 1. Channels 3–5 were actually of identical curvature ($D/h \simeq 20$) and only differed by the relative width b/h. Channels 1, 2 and 6–9 differed essentially by the curvature parameter D/h. Rough channel 10 was geometrically similar to smooth channel 5.

The local heat transfer was determined in heating either the concave surface (of the outer tube) or the convex surface (of the calorimetric foil). To ascertain a convective component of the heat flux, account was

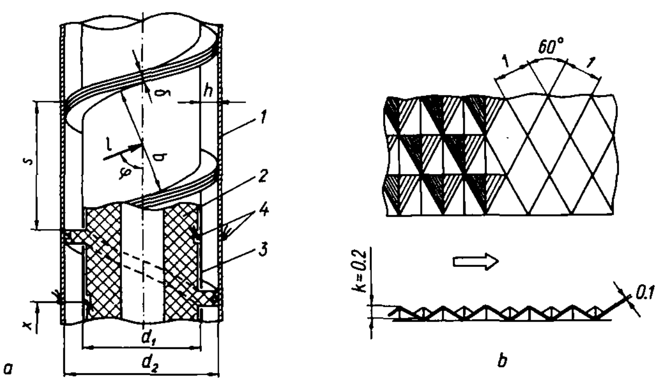

FIG. 1. Fragments of a helical channel (a) and a rough foil (b): 1, outer calorimetric tube; 2, worm insertion; 3, calorimetric foil; 4, thermocouples.

Table 1. The basic geometric characteristics of the channels studied

Channel no.	s (mm)	b (mm)	h (mm)	φ (deg)	D/h	b/h
1	30	25.6	6.05	72.4	5.5	4.2
2	70	54.5	3.95	55.3	12.1	13.8
3	120	9.9	4.05	40.0	19.2	2.4
4	120	74.2	4.0	40.0	19.4	18.5
5	120	22.8	3.85	40.2	20.1	5.9
6	180	36.4	4.0	29.2	33.4	9.1
7	231	37.8	4.03	23.6	50.2	9.4
8	192	28.2	2.0	29.2	71.9	14.1
9	250	19.5	2.65	22.8	84.2	7.4
10	120	20.9	3.5	40.5	22.1	6.6

taken of the radiative heat transfer between the convex and concave surfaces, heat losses to the ambient and longitudinal heat flows along the channel walls. The investigation was conducted under the boundary conditions approaching q_w = const. Hydraulic drag in the helical channels was estimated from the static pressure drop over a definite length and expressed as the total drag due to the wall friction along the entire channel perimeter and due to the momentum variation.

The experimental data processing for each helical channel was reduced to obtaining the Nu, Re and ξ values, to finding the dependence of Nu and ξ on Re and, eventually, to unifying the results for all channels. The local mean mass temperature of flow T_f was taken to be the reference temperature, the local mean mass velocity u_f was assumed to be the reference velocity and the double height of the channel $2h$ was taken as the reference dimension in studying heat transfer or the equivalent channel diameter d_e in studying hydraulic drag:

$$d_e = \frac{4f}{\Pi} = \frac{2(s-\delta)\sin\varphi \times h}{(s-\delta)\sin\varphi + h}. \quad (1)$$

The mean curvature diameter D and the mean swirling angle φ of the helical channel were obtained from the standard equations

$$D = \frac{0.5(d_1+d_2)}{\sin^2\varphi} \quad (2)$$

$$\varphi = \arctan\left[\frac{0.5\pi(d_1+d_2)}{s}\right]. \quad (3)$$

A detailed description of the investigation technique and data processing, as well as results of some methodical experiments, can be found in ref. [10].

The analysis of the experimental errors revealed that, for the most part, the relative errors of Nu were 2–3%, those of Re were 3–7%, those of ξ were as large as 3–5%, and only at smaller Re values ($Re \leqslant 2\times10^3$) did the Nu errors reach 10%.

3. RESULTS

3.1. *Local heat transfer*

The present subsection considers the results regarding heat transfer in smooth helical channels, obtained in the region of stabilized heat transfer for Re varying from 10^3 to 2×10^5. As is evident from Figs. 2 and 3, heat transfer from the concave surface is greater than that from the convex surface within almost the entire Re range studied. Only in the channel 3 (D/h = 19.2), when $Re < 4\times10^3$, and in channel 8 (D/h = 71.9) with $Re > 3\times10^4$, is it similar for both the surfaces. In the region of developed turbulent flow, the maximum enhancement of heat transfer from the concave surface as against that in the straight tube amounts to 60%, whereas its maximum reduction for the convex surface is equal to 50%.

Investigations disclosed that the relative width of the channel b/h (especially when $b/h \gtrsim 6$) insignificantly affects the heat transfer rate in the midwidth of each surface (Fig. 2). The same conclusion ensues from ref. [12] in analysing the hydraulic drag in curved channels. The most appreciable influence on the local heat transfer of the helical channels is exerted by the relative curvature D/h. With an increase in the channel curvature (a decrease in the parameter D/h), heat transfer from the convex surface is markedly reduced, whereas that from the concave surface is enhanced (Fig. 3).

Based on the heat transfer data, laminar-vortex, transient and turbulent flows are discriminated. It is

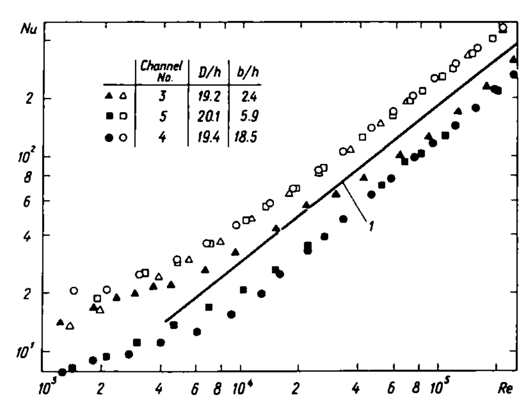

FIG. 2. The effect of the parameter b/h on heat transfer from convex (solid dots) and concave (clear dots) surfaces of helical channels at $D/h \simeq 20.1$ by equation (9) for the tube heat transfer in turbulent flow.

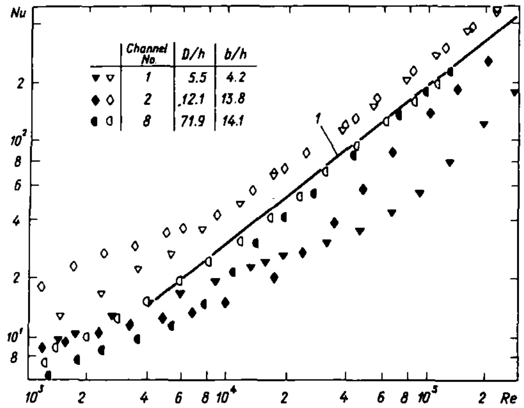

FIG. 3. The effect of the parameter D/h on heat transfer from convex and concave surfaces of helical channles. Designation as in Fig. 2.

characteristic of the helical channels that the transition to turbulent flow occurs at *Re* values larger than those in the straight channels, and the transition is smooth rather than stepwise. Moreover, in the large-curvature channels, the transition to turbulent flow on the concave and convex surfaces takes place at different *Re* values and the lengths of the transition zone differ. Thus, in channel 2 ($D/h = 12.1$), the transition to turbulent flow on the concave surface occurs at $Re \simeq 10^4$ and, on the convex surface, it takes place at $Re \simeq (1\text{–}6) \times 10^4$ (Fig. 3). In channel 1, with the greatest curvature ($D/h = 5.5$), it occurs on the concave surface at $Re \simeq (1\text{–}2) \times 10^4$, whereas on the convex surface, the transition only starts at $Re \simeq 6 \times 10^4$ and fully developed turbulent flow does not set in within the range of *Re* values studied.

Such qualitative variations of the flow regimes in the helical channels verify the investigations of the shear stress and its fluctuations at the wall along the perimeter of the coil pipe [13], as well as the measurements of the velocity profiles (Fig. 4) and Reynolds

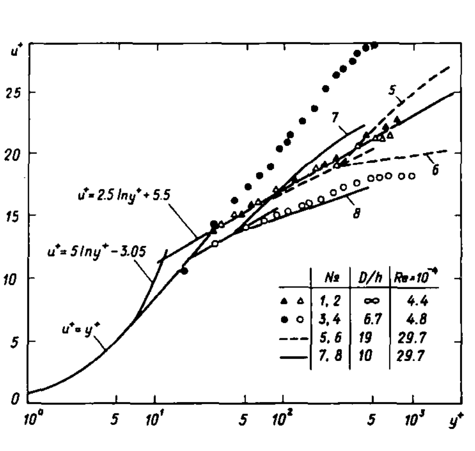

FIG. 4. The velocity profiles on convex (1,3 (solid dots), 5,7) and concave (2,4 (clear dots), 6,8) surfaces of helical channels: 1–4, data of ref. [14]; 5,6, data of ref. [15]; 7,8, data of ref. [16].

stresses on the concave and convex surfaces in curved channels of different curvatures [14]. As seen from Fig. 4, with an increase in channel curvature, deviations of the velocity profiles from the standard logarithmic law occur at smaller y^+ values. While the experimental data for $D/h = \infty$ actually obey the logarithmic law, the velocity profiles at $D/h = 6.7$ decline downwards with distance from the concave surface, whereas at a distance from the convex surface, they deviate upwards, which indicates, correspondingly, the flow turbulence and a decrease in the turbulent transfer rate. The Reynolds stresses on the convex surfaces of the helical channels are noticeably smaller and those on the concave surfaces, and are somewhat larger than in the straight plane channel. Besides, they decrease and approach zero on the convex surfaces as the channel curvature increases, which is also indicative of turbulent transfer reduction.

These phenomena, observed in the course of studying the thermohydraulic characteristics in individual helical channels with the heat transfer agent flow in the field of mass forces, are attributed to the emergence of secondary flows differing in their nature from normal turbulence. Many authors [1, 17, 18] mostly differentiate between two types of secondary flow originating in curvilinear channels, near the end walls and the so-called Taylor–Görtler vortices, on the concave walls. The initiation and rate of secondary flows of either or both types are dependent simultaneously on the operating conditions and geometric parameters.

3.2. *Hydraulic drag*

Hydraulic drag in the helical channels is studied for *Re* values ranging from 10^2 to 2×10^5. Within the entire *Re* range, it is possible to distinguish laminar, laminar-vortex and turbulent flows (Fig. 5). In contradistinction to the straight channels, the transition from one flow to another in the helical channels is smooth; therefore, there are no clear boundaries of the transition. Moreover, the effect of the geometric parameters b/h and D/h on hydraulic drag is less pronounced than that on heat transfer. In laminar flow, the hydraulic drag of each helical channel practically conforms to the hydraulic drag of the straight plane channel [19] with the same ratio b/h. In laminar-vortex flow, as the parameter D/h increases (the channel curvature decreases), the hydraulic drag in the helical channels decreases. In turbulent flow, the hydraulic drag does not actually depend on the geometric parameters. Besides, in channels 1, 3 and 5 with the minimum relative width b/h equal, respectively, to 4.2, 2.4 and 5.9 (Table 1), self-similarity of hydraulic drag with respect to *Re* is obtained at $Re \gtrsim 5 \times 10^4$ ($\xi \simeq 0.03$). This fact is also reported in ref. [2] for curved channels with commensurable lengths of the cross-section sides at $Re \gtrsim 8 \times 10^4$.

Transient flow identified by the heat transfer data for the helical channels is not distinctly defined from the hydraulic drag results; rather it sort of merges with turbulent flow.

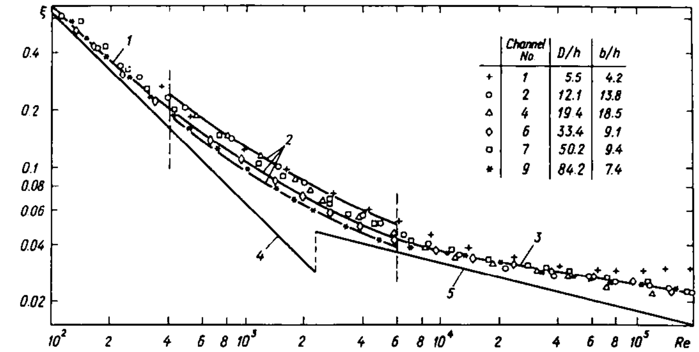

FIG. 5. Hydraulic drag in helical channels: 1–3, by equations (16)–(18), respectively; 4, by the Hagen–Poiseuille equation for a tube in laminar flow ($\xi = 64/Re$); 5, by the Blasius equation for a tube in turbulent flow ($\xi = 0.3164/Re^{0.25}$).

4. CORRELATION OF RESULTS

4.1. *Flow regimes*

Sorting out the experimental data on heat transfer and hydraulic drag necessitates a clear delimitation of the regions of separate flows. Based on the data pertaining to the local heat transfer from the convex and concave walls of the helical channels, effort is made to obtain relations for Re_{cr} on individual surfaces. It is difficult to clearly ascertain the beginning (Re_{cr1}) and the end (Re_{cr2}) of the transition from laminar-vortex flow to turbulent flow on the concave surface; therefore, a certain mean Re_{cr} value is determined from the relation (Fig. 6, curve 1)

$$Re_{cr} = 2300+1400\exp[4.5(D/h)^{-0.3}]. \quad (4)$$

Re_{cr1} and Re_{cr2} on the convex surface can be estimated inasmuch as the heat transfer rate over the Re range considered changes in character twice (Fig. 3). To find Re_{cr1} on the convex surface, the following correlation is obtained (curve 2):

$$Re_{cr1} = 2300+2340\exp[22(D/h)^{-1.1}] \quad (5)$$

and Re_{cr2} is defined by the relation (curve 3)

$$Re_{cr2} = 2300+207\,000\exp[42\,500(D/h)^{-4}]. \quad (6)$$

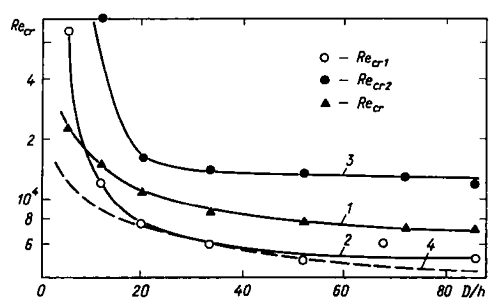

FIG. 6. Dynamics of Re_{cr} on separate surfaces of helical channels: 1–3, by equations (4)–(6), respecively; 4, Re_{cr} for a coil [20].

It should be pointed out that the most marked alterations in the transition character for the convex and concave surfaces of the helical channels are observed when $D/h < 20$. Qualitatively similar results were found in ref. [20] for coils.

4.2. *Heat transfer in turbulent flow*

All flows at Re larger than Re_{cr} (equation (4)) for the concave surface and at Re larger than Re_{cr2} (equation (6)) for the convex surface refer to turbulent flows. In sorting out the results, experimental data were normalized on the basis of heat transfer in the straight plane channel. Heat transfer was expressed as that in the annulus with one-sided heating at $d_1/d_2 = 1$ [21]:

$$Nu_0/Nu_t = 1-\varphi(Pr), \quad (7)$$

where $\varphi(Pr) = 0.45/(2.4+Pr)$. In the given case, $Pr = 0.71$; therefore

$$Nu_0 = 0.86Nu_t, \quad (8)$$

where Nu_t is the stabilized heat transfer in the tube defined by the expression [22]

$$Nu_t = 0.0225Re^{0.8}\,Pr^{0.6}. \quad (9)$$

With such data interpretation employed, the correlation of stabilized heat transfer ($l/2h > 60$) for turbulent flow in helical channels depending on their curvature is presented in Fig. 7. While heat transfer

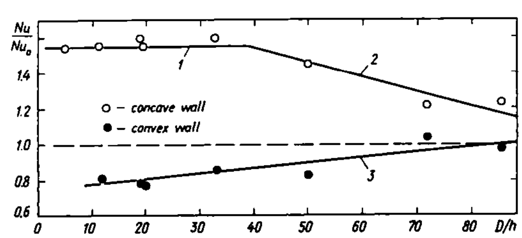

FIG. 7. The relative heat transfer of convex and concave surfaces of helical channels in turbulent flow: 1–3, by equations (10) and (11), respectively.

Table 2. The coefficients c and m in equation (12) for various channels

Channel no.	D/h	Convex wall		Concave wall	
		c	m	c	m
1	5.5	0.70	0.37	0.098	0.66
2	12.1	1.75	0.23	0.96	0.42
3	19.2	0.83	0.40	0.26	0.55
4	19.4	0.93	0.30	0.88	0.42
5	20.1	0.31	0.45	0.36	0.52
6	33.4	1.54	0.25	0.41	0.49
7	50.2	0.95	0.30	0.44	0.47
8	71.9	0.63	0.33	0.124	0.58
9	84.2	1.43	0.25	0.34	0.47

from the convex wall gradually decreases with an increase in the channel curvature (a decrease in D/h), heat transfer from the concave wall gradually increases with D/h decreasing to $\simeq 40$ and does not actually vary with a further increase in the channel curvature. The results are generalized by the following relations:

for the concave wall (Fig. 7, curves 1, 2)

$$\frac{Nu}{Nu_0} = \begin{cases} 1.55 & \text{when } 5 < D/h \leqslant 40 \\ 1.55-0.008(D/h-40) & \text{when } 40 < D/h < 90; \end{cases} \quad (10)$$

for the convex wall, when $10 < D/h < 90$ (curve 3)

$$Nu/Nu_0 = 0.75+0.003D/h. \quad (11)$$

4.3. *Heat transfer in laminar-vortex flow*

Laminar-vortex flows are those at $Re < Re_{cr}$ (equation (4)) for the concave surface and those at $Re < Re_{cr1}$ (equation (5)) for the convex surface. The heat transfer data for the concave and convex walls of each channel are generalized by relations of the type

$$Nu = c \times Re^m, \quad (12)$$

where the constants c and m are given in Table 2. As follows from Table 2, there is no strict regularity in the variation of c and m depending on the channel curvature. However, for the convex wall, it is possible to obtain the unique correlation

$$Nu = 1.4Re^{0.3}(D/h)^{-0.1}. \quad (13)$$

4.4. *Heat transfer in the transition from laminar-vortex to turbulent flow*

To describe heat transfer in tubes in the transition region, use is generally made of the intermittence coefficient γ, defined as the ratio of the time of turbulent flow existence at the measurement point to the total time of observation. Therefore, it can be assumed that $\gamma = 0$ at Re_{cr1} and $\gamma = 1$ at Re_{cr2}. In correlating data on local heat transfer in the transition region of the tube, ref. [23] successfully employed a relation of the type

$$Nu = Nu_L(1-\gamma)+Nu_T\gamma, \quad (14)$$

where Nu_L and Nu_T are the laminar and turbulent flow heat transfer, respectively. To describe the alteration of γ, use is made of the relation

$$\gamma = \frac{Re-Re_{cr1}}{Re_{cr2}-Re_{cr1}}. \quad (15)$$

The laminar-vortex flow heat transfer should, naturally, be used as Nu_L in the helical channels.

Comparing heat transfer from the convex walls of some channels, which is predicted by relations (11), (13) and (14), with experimental data indicates fairly good agreement (Fig. 8).

4.5. *Hydraulic resistance*

Owing to the fact that, according to the data of hydraulic drag in helical channels (Fig. 5), there are no distinct boundaries between separate flows, they are determined roughly. The results are generalized by the following correlations:

for laminar flow with $Re = 10^2$–4×10^2 (Fig. 5, curve 1)

$$\xi = (1.68 \log Re-2.16)^{-2}; \quad (16)$$

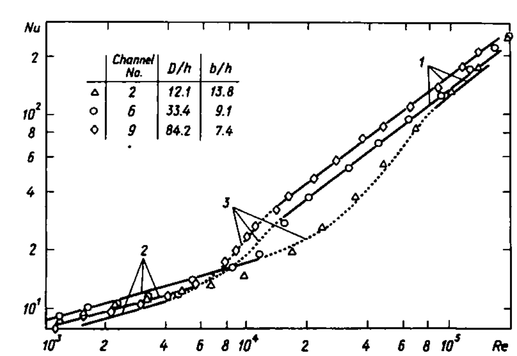

FIG. 8. Comparison of heat transfer from a convex surface of a helical channel in different flows with prediction by correlations: 1–3, by equations (11), (13) and (14), respectively.

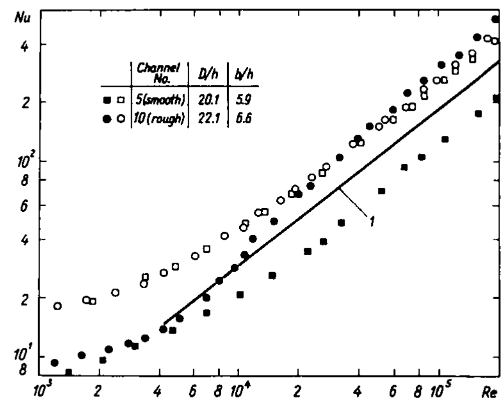

FIG. 9. The heat transfer enhancement in a helical channel. Clear dots pertain to a concave surface and solid dots pertain to a convex surface: 1, by equation (9) for the tube heat transfer in turbulent flow.

for laminar-vortex flow with $Re = 4\times10^2$–6×10^3 (curve 2, $D/h = 10$, 35 and 70, respectively)

$$\xi = 1.71(D/h)^{-0.15}(2.25\log Re - 3.65)^{-2}; \quad (17)$$

for turbulent flow with $Re = 6\times10^3$–2×10^5 (curve 3)

$$\xi = (1.24\log Re + 0.17)^{-2}, \quad (18)$$

with the exception of channels 1, 3 and 5 of the minimum relative width b/h (equal, respectively, to 4.2, 2.4 and 5.9), where $\xi \simeq 0.03$ at $Re \gtrsim 5\times10^4$.

5. METHODS OF HEAT TRANSFER ENHANCEMENT

To enhance heat transfer from an inefficient convex surface of helical channels, the surface is made rough (Fig. 1(b)). As is clear from Fig. 9, heat transfer from smooth concave surfaces of rough (10) and likewise fully smooth (5) helical channels coincides virtually over the entire Re range and, in the turbulent flow region ($Re \gtrsim 10^4$), exceeds heat transfer from a circular straight tube by 30–35%.

Heat transfer from the convex surfaces of the corresponding helical channels differs slightly only at Re values of up to 5×10^3. Subsequently, with Re increasing up to 2×10^4, heat transfer from the rough convex surface increases noticeably, i.e. roughness manifests itself partially, whereas in the developed turbulent flow ($Re > 2\times10^4$), when roughness is displayed completely, it reaches and even exceeds heat transfer from the concave surface. In developed turbulent flow, heat transfer from the rough convex surface is twice as large as that from the smooth convex surface. Despite the adverse effect of centrifugal forces on the convex surface heat transfer, this conforms to its maximum enhancement attained in the rough annuli in the zone, where roughness manifests itself fully [11].

No considerable difference between hydraulic drag in the rough and smooth helical channels has been observed (Fig. 10). Hydraulic drag of both channels in laminar and laminar-vortex flows actually coincides. Only in turbulent flow, when $Re > 2\times10^4$, is some increase of hydraulic drag with its subsequent shift to self-similarity with respect to Re ($\xi \simeq 0.41$) noticed. The fact that hydraulic drag in the rough and smooth helical channels varies insignificantly, whereas heat transfer is enhanced markedly, is evidence of the great energy efficiency of such channels with artificial roughness applied to the convex surface.

When evaluating the heat transfer enhancement in all the considered helical channels by the generally accepted efficiency parameters $\overline{St}^3/\xi$ and $(\overline{St}/St_0)/(\xi/\xi_0)$, it must be noted that, for $Re \gtrsim 10^4$, the most efficient heat transfer is of moderature-curvature channels 4, 6 and 10 ($D/h = 19.4$, 33.4 and 22.1, respectively), and the least efficient heat transfer is of large- and small-curvature channels 1 and 9 ($D/h = 5.5$ and 84.2).

6. CONCLUSIONS

1. It is established experimentally that, with an increase in helical channel curvature, heat transfer from the concave surface is enhanced (by up to

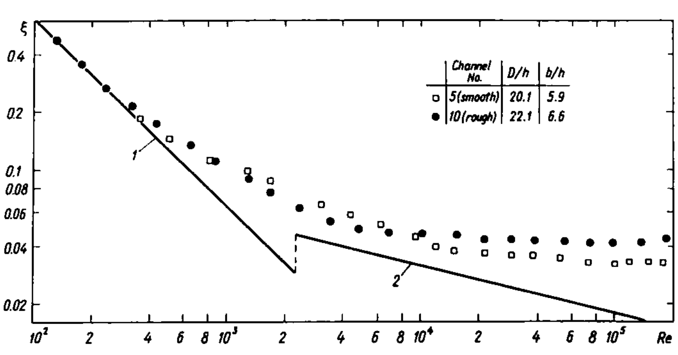

FIG. 10. Hydraulic drag in smooth (clear dots) and rough (solid dots) helical channels: 1,2, by equations for a tube in laminar ($\xi = 64/Re$) and turbulent ($\xi = 0.3164/Re^{0.25}$) flows, respectively.

60%) and that from the convex surface is reduced (by up to 50%) relative to heat transfer in the straight tube.

2. The transition to turbulent flow occurs at *Re* values greater than those in straight channels and at different *Re* values on the concave and convex surfaces, and the transition zone has different lengths.

3. Correlations are obtained to determine the critical Reynolds numbers for the transition to turbulent flow on the concave and convex surfaces (equations (4)–(6)), heat transfer from the concave and convex surfaces in turbulent, laminar-vortex and transient flows (equations (10), (11), (13) and (14)) and hydraulic drag in the helical channels (equations (16)–(18)).

4. Comparison of the results shows that the heat transfer enhancement method, combining flow swirling and turbulization with the artificial roughness on the convex wall, can be considered as highly efficient.

REFERENCES

1. V. K. Shchukin, *Heat Transfer and Hydrodynamics of Internal Flows in the Fields of Mass Forces*. Izd. Mashinostroyeniye, Moscow (1980).
2. B. P. Ustimenko, *Turbulent Transfer Processes in Rotating Flows*. Izd. Nauka, Alma-Ata (1977).
3. V. K. Shchukin and V. A. Filin, Convective heat transfer in short curvilinear channels, *J. Engng Phys.* **12**(2), 169–176 (1967).
4. J. W. Yang and N. Liao, Turbulent heat transfer in rectangular ducts with 180°-bend, *Heat Transfer 1974, Proc. 5th Int. Heat Transfer Conf.*, Vol. 2, pp. 169–172, Tokyo (1974).
5. N. Seki, S. Fukusako and M. Yoneta, Heat transfer from the heated concave wall of a return bend with rectangular cross section, *Wärme- und Stoffübertragung* **17**(1), 17–26 (1982).
6. N. Seki, S. Fukusako and M. Yoneta, Turbulent heat transfer characteristics along the heated convex wall of a rectangular cross-sectional return bend, *Wärme- und Stoffübertragung* **17**(2), 85–92 (1983).
7. I. I. Telegina, Study of heat transfer and hydraulic drag in the curved channels of rectangular cross section, Candidate Thesis (Engng), Moscow (1976).
8. F. Kreith, The influence of curvature on heat transfer to incompressible fluids, *Trans. ASME* **77**(8), 1247–1256 (1955).
9. V. M. Šimonis, P. S. Poškas and J. V. Vilemas, Local heat transfer coefficients and pressure drop in air flow through helical annular ducts, *Heat Transfer—Sov. Res.* **19**(6), 92–102 (1987).
10. V. M. Šimonis, V. P. Šukys and P. S. Poškas, Thermohydraulic properties (coefficients of local heat transfer and hydraulic drag) of helical channels (1. Experimental unit, procedure and preliminary experiments), *Fluid Mech.—Sov. Res.* **18**(4) (1989).
11. J. V. Vilemas and V. M. Šimonis, Heat transfer and friction of rough ducts carrying gas flow with variable physical properties, *Int. J. Heat Mass Transfer* **28**, 59–68 (1985).
12. A. J. Ward Smith, The flow and pressure losses in smooth pipe bends of constant cross section, *J. R. Aeronaut. Soc.* **67**(631), 437–448 (1963).
13. V. A. Mikaila, P. S. Poškas and J. V. Vilemas, The local shear stress on the coil pipe wall (2. The effect of the coil curvature), *Trudy AN Lit. SSR, Ser. B* **3**(166), 115–119 (1988).
14. J. Vilemas and P. Poškas, Heat transfer in helical channels with strong curvature, *Heat Transfer 1990, Proc. 9th Int. Heat Transfer Conf.*, Vol. 3, pp. 369–373, Jerusalem (1990).
15. S. Eskinazi and H. Yeh, An investigation on fully developed turbulent flows in a curved channel, *J. Aero. Sci.* **23**, 23–24 (1951).
16. F. L. Wattendorf, A study of the effect of curvature on fully developed turbulent flow, *Proc. R. Soc.* **148**, 565–598 (1935).
17. P. D. McCormack, H. Welker and M. Kelleher, Taylor–Görtler vortices and their effect on heat transfer, *Trans. ASME, J. Heat Transfer* **91**(2), 101–112 (1970).
18. M. D. Kelleher, D. L. Flentie and R. J. McKee, An experimental study of the secondary flow in a curved rectangular channel, *Trans. ASME, J. Fluid Engng* **102**(1), 92–96 (1980).
19. J. P. Hartnett, J. C. Y. Koh and S. T. McComas, A comparison of predicted and measured friction factors for turbulent flow through rectangular ducts, *Trans. ASME, J. Heat Transfer* **84**(1), 101–108 (1962).
20. Yu. V. Krasnoukhov and Ye. D. Fedorovich, Hydraulic drag of helical coils with one-phase and two-phase flows. In *Improvement of the Heat Transfer Efficiency in Energy Equipment* (Edited by Ye. D. Fedorovich), pp. 104–116. Izd. Nauka, Leningrad (1981).
21. B. S. Petukhov and L. I. Roizen, Correlations for heat transfer in annular tubes, *Teplofiz. Vysok. Temp.* **12**(3), 565–569 (1974).
22. V. A. Kurganov and B. S. Petukhov, Analysis and unification of experimental data on heat transfer in tubes in turbulent flow of gases with variable properties, *Teplofiz. Vysok. Temp.* **12**(2), 304–315 (1974).
23. V. E. Kaupas, P. S. Poškas and J. V. Vilemas, Heat transfer to a transition-range gas flow in a pipe at high heat fluxes. 2. Heat transfer in laminar to turbulent flow transition, *Heat Transfer—Sov. Res.* **21**(3), 340–351 (1989).